Visualizing Structural Health Monitoring of CF Composites Through Electroluminescence

J. Qiu[1], M.K. Idris[2], G. Grau[2], G.W. Melenka [1]*
[1] Mechanical Engineering, York University, Toronto, Canada
[2] Electrical Engineering and Computer Science, York University, Toronto, Canada
* Corresponding author (gmelenka@yorku.ca)

ABSTRACT

Conventional damage inspection methods and characterization of carbon fibre (CF) composites are typically destructive, expensive, and do not provide spatial resolution. In this work, non-destructive monitoring of CF composites is presented with an intrinsic electroluminescent (EL) thin-film epoxy resin-phosphor membrane sandwiched between semi-transparent CF mesh and woven CF fabric lamina. Different damage states in the CF composite cause EL luminance gradients which allows for visual inspection and damage detection of the CF composite at specified locations. The proposed methodology offers simple and effective structural health monitoring to any product constructed from CF ranging from aerospace to high performance sporting goods.

KEYWORDS: *Structural Health Monitoring, Electroluminescence, Carbon Fibre Textile Composite*

1 INTRODUCTION

Carbon fibre (CF) is known for its high strength-to-weight ratio, mechanical and thermal properties, and most importantly its electrical conductivity.(Zhu et al. 2014). However, CF stand alone is unable to adapt to wide range of applications, thus, a reinforcing material is required. Furthermore, textile composites are a form of composite structures where yarns are interwoven to create a textile architecture.(Bilisik K 2017) They have improved damage resistance over conventional unidirectional composite structures. Together, these properties have made CF reinforced composite one of the strong candidates for advanced aerospace and civil structural application.

Despite the advantages of composite materials, the failure mechanics is difficult to predict. A major challenge for CF textile composites is strain measurement. Textile composites exhibit a heterogenous structure that produces anisotropic variation in strain and complex failure mechanics.(Cai et al. 2012) Thus, careful selection of devices such as strain gages must be considered when assessing textile composites structures. (Lang and Chou 1998)

The conventional damage evaluation methods rely on destructively examination the specimen which is not suitable for in-service applications. Thus, non-destructive damage evaluation method is required. Common inspection methods for composites include X-Ray, ultrasonic inspection, Bragg Grating or eddy currents. (Zhu et al. 2011)

Structural Health Monitoring (SHM) implements damage detection and failure prognosis within engineering structures. SHM is the most suitable for CF reinforced composites since it removes processing cost and time, is non-destructive, and does not require expensive external measuring equipment. This process aims to replace periodic maintenance inspection and avoid catastrophic failures by relying on continuous real-time monitoring.

In this work, the conductive nature of CF will be exploited to integrate SHM elements within advanced textile composite structures.

There are numerous SHM sensors existing in the current market to measure structural parameters variation such as stress, strain, temperature, humidity and many more. Resistance strain gages utilize the strain-resistance effect on a conductor and external amplification circuits to monitor the strain state of the specimen. Piezoelectric sensors convert stress field variation of the material to electric charge accumulation or electric field. For cracking, the variations in thickness or defects interrupt and alter the pattern of eddy current. However, all these sensors either rely on external components which can cause significant complication in manufacturing, measurement accuracy and calibration, or have discrete sensor elements in which only the properties of the area of interest is accounted for.(Cai et al. 2012)

The goal of this work is to investigate a novel method to integrate damage sensing and visualization in CF composites, specifically textile CF reinforced composites, utilizing the conductive nature of CF and capacitive coupling between laminates and their correlation between geometric changes in the composite.

The failure state of a CF reinforced composite can be quantified by its electrical properties. (Xia and Curtin 2008) We achieve self-visualization of the damage by utilizing the physical phenomenon of electroluminescence (EL). Alternating current electroluminescence (ACEL) is an electro-optical phenomenon in which a phosphor emits light in response to a strong AC electric field. The luminance of the EL mode directly correlates to the resistance of the electrodes and the capacitance of the device. EL SHM not only senses the damage state of the CF composite but also visualizes it as luminance variation.

EL research and commercial products have focused on applications such as portable lighting, displays, smart wearable electronics, and signage. Despite difference in geometry and size, these devices commonly use a thin-film configuration consisting of two electrodes separated by a dielectric phosphor membrane. One or both of the electrodes are transparent to allow light to escape. There are multiple ways to construct the same configuration, specifically, the geometry can vary while the stacking configuration remains unchanged. For instance, Liang et al fabricated coaxial flexible ACEL fibres for wearable electronic.(Liang et al. 2017) Conventionally, EL panels are fabricated using indium tin oxide (ITO) on glass substrate as the transparent electrode; however, this is not compatible with CF composite manufacturing process.

Here, a novel ACEL SHM epoxy reinforced CF composite is demonstrated. The stack consists of a semi-transparent CF mesh electrode, dielectric phosphor membrane consisting of ZnS: Cu particles dispersed in epoxy resin, and a woven CF fabric electrode encapsulated by epoxy resin. The structure is designed and fabricated using standard composite fabrication protocols and materials. Mechanical testing in the form of 3-point bending demonstrates the performance of the manufactured ACEL damage-self-sensing and visualization by the epoxy reinforced CF composite structure.

2 METHODOLOGY

2.1 Specimen Fabrication

A schematic of the fabricated ACEL structure is shown in Figure 1. This figure shows both the textile structure as well as a cross-section of fabricated structure.

(a) (b)

Figure 1 Internal composition of Fabricated Structure in illustrated schematic: (a) 40x Magnification showing composition of structure, (b) 10x Magnification allows precise identification of weft and warp shown as dark ellipse and undulating bands respectively

In the interest of the mechanical testing process, ASTM D2344 short beam three-point bending standard will be modified and referenced for flexible laminate. Specifically, 25.4mm by 80mm laminate will by fabricated.(Laminates 2000) A schematic of the fabricated sensing structure is shown in Figure 2.

The operational protocol on fabrication of the ACEL epoxy reinforced CF laminate can be broken down to its corresponding components: semi-transparent epoxy resin infused CF mesh lamina, ZnS: Cu-epoxy resin membrane, and epoxy resin infused woven CF fabric lamina. The smooth epoxy resin infused woven CF fabric lamina is first fabricated as the substrate for the ZnS: Cu-epoxy resin membrane to coat uniformly and the semi-transparent epoxy resin infused CF mesh lamina is overlaid on top subsequently. Ultimately the specimen is encapsulated with epoxy resin.

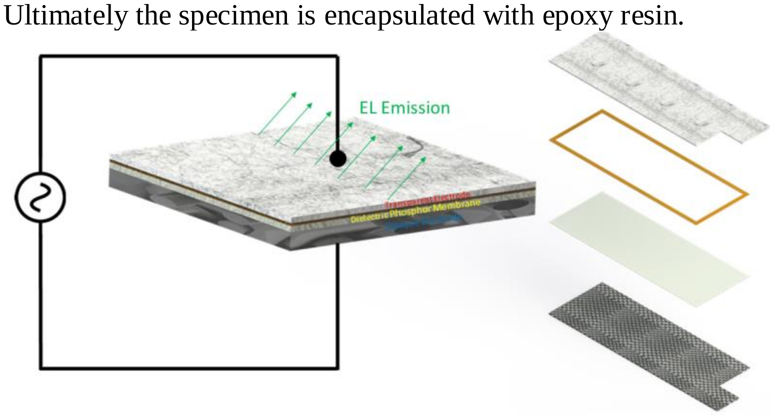

Figure 2 Overview of EL-CF Structure and its components: (a) Semi-transparent epoxy resin infused CF mesh as Transparent Electrode, (b) ZnS: Cu-epoxy resin membrane as Dielectric Phosphor Membrane, Kapton tape boundary as shorting prevention layer and (c) epoxy resin infused woven CF fabric as Opaque Electrode.

The full fabrication schematics for epoxy resin infused woven CF fabric lamina, ZnS: Cu-epoxy resin membrane, and epoxy resin infused CF mesh lamina are illustrated in Figure 3, 4, 5 respectively along with fabrication specification provided in Table 1.

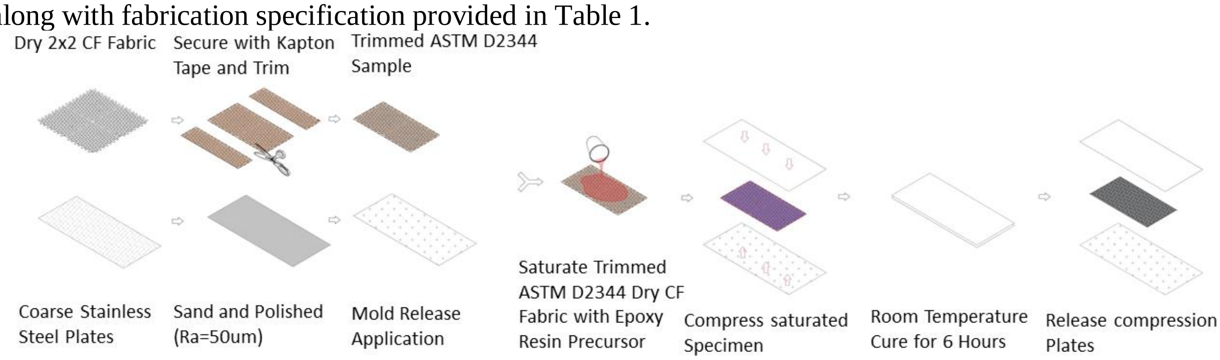

Figure 3 Fabrication process of epoxy resin infused woven CF lamina

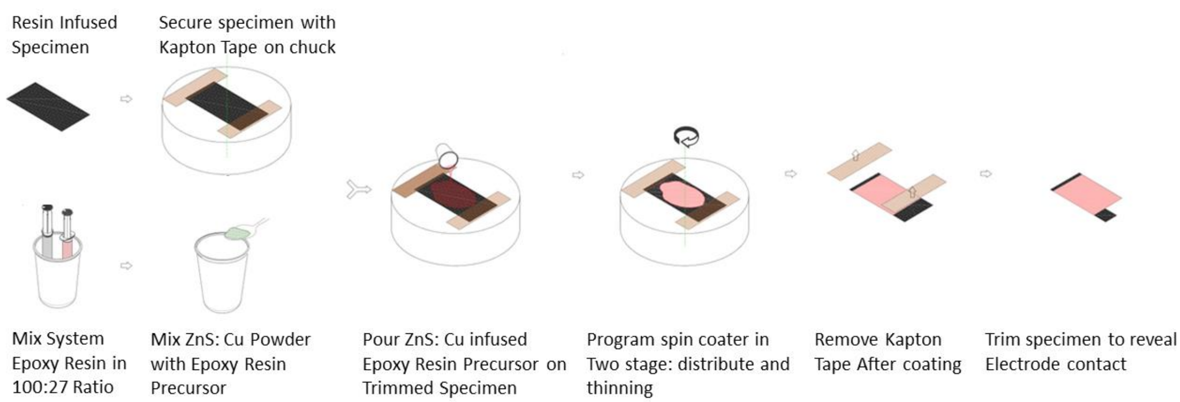

Figure 4 Fabrication Procedure of ZnS: Cu-epoxy resin membrane s

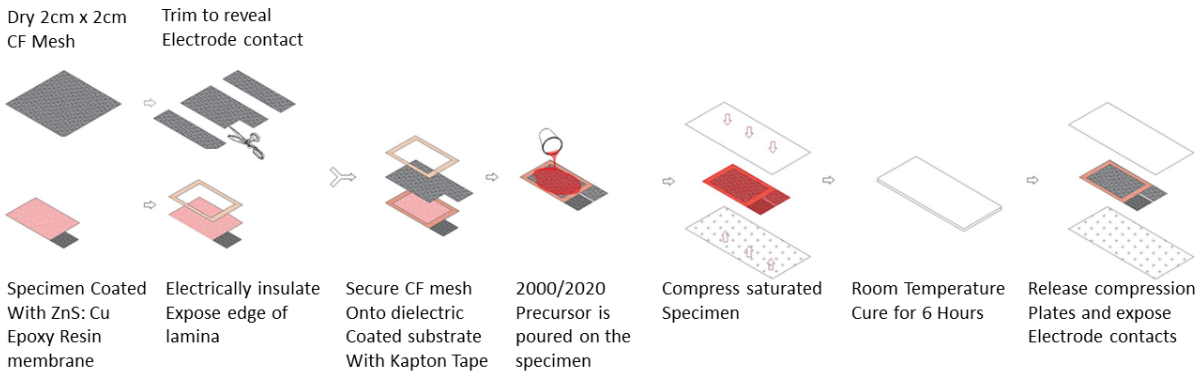

Figure 5 Assembling procedure of the EL-CF structure

Table 1 Material specification for fabrication

Component	Detail
CF Fabric	PAN base 2x2, 90-degree Weave CF Fabric (3k Bundle)
Epoxy Resin and Encapsulation	Fibre Glast 2000/2020 System Epoxy Resin
Mold Release	Frekote 700-NC
Compression Plates	3.5”x15” US32D Satin Stainless-Steel Plates
Phosphor Powder	Shanghai Dongzhou Industrial CO., LTD Model D502-B ZnS: Cu Powder
CF Mesh	Canada Composite 10g, 35”x78” Carbon Veil
Electrical Insulating Boundary	ULINE 1 Mil, 1”x36 yds Kapton Tape

2.2 Structural Characterization

Prior to utilizing the manufactured structure as a health monitoring device, the EL luminance control parameters were characterized. The characterization of the manufactured EL sensor entailed thickness measurement using both optical (Bruker Contour GT-X) and stylus (KLA Tencor Alphastep D500) profilometer; geometry measurement with an optical microscope, resistance and capacitance measurement utilizing a Parameter Analyzer (Keithley 4200a Parameter Analyzer) and luminescence measurement using an optical machine vision camera (Basler acA2440-35µm) with EL strip (Adafruit Aqua EL strip tape) as luminance coefficient calibration.

The EL luminance of the manufactured structure is controlled by three key parameters): (1) Resistivity (ρ) of CF-fabric epoxy structure, (2) thickness (t) and uniformity of the dielectric phosphor membrane, (3) applied voltage (ΔV).

The varying control parameters of both woven CF fabric-epoxy resin electrode and CF mesh-epoxy resin electrode are the sheet resistance, and the surface finish. Surface finish of the electrode substrate directly corresponds to the uniformity of the membrane. Resistivity is directly proportional to EL luminance, whereas the surface finish, controls the uniformity of luminance. According to Equation 1, the resistivity of the electrodes is quantified by first quantifying electrodes thickness through cross-sectional microscopy, then utilizing Van der Pauw method with Keithley 4200a Parameter Analyzer in both resin infused and natural states. The Van der Pauw test specimens (64mm by 64mm square) are fabricated by extrusion printing conductive silver ohmic contacts (4mm by 4mm square) on the edge of a square specimen with a Voltera V-One PCB printer and conductive silver polymer ink prior to epoxy application.

$$\rho_{symmetric} = \frac{\pi t R_{12,34}}{\ln(2)} \tag{1}$$

The EL luminance control parameters for ZnS: Cu-epoxy resin membrane are the dielectric-phosphor ratio, membrane thickness, and substrate surface finish. The mixing ratio between epoxy resin and ZnS: Cu powder directly influences precursor viscosity, dielectric constant, and luminance density. As the spin coating speed and precursor viscosity strongly correlated to the membrane thickness, a tradeoff exist between dielectric-phosphor ratio and membrane thickness to achieve maximum luminance. Membrane thickness was measured by stylus profilometer and the dielectric constant was determined by capacitance measurement (CV and CF curve) on Keithley 4200a Parameter Analyzer. Finally, the surface finish of the epoxy resin infused woven CF fabric is quantified with a Bruker Contour GT-X optical profilometer.

2.3 Mechanical Testing

As the intrinsic ACEL is an electric field induced illumination mechanism. Corresponding to the resistivity variation of the electrodes and capacitive or electric field intensity variation, the damage and strain state of the fabricated structure can be sensed, and the fibre elongation and dielectric thickness reduction quantified. Mechanical testing was performed to examine the variation in EL luminance as the function of mechanical strain using a modified ASTM D2344 short beam three point bending test.(Laminates 2000) This mechanical experimental apparatus assembly consist of three main components: mechanical stress input, deformation deflection capture, and EL luminance capture to simultaneously capture and generate relations among stress, deflection, and EL luminance.

The mechanical input stress is delivered by a manual hydraulic press with the addition of 3-Point bending testing fixture. To accurately monitor the applied force, a microcontroller (Arduino Uno) is coupled with a load cell (34mm x 34mm x 7.8mm) rated for a maximum force of 50kg at the junction between the hydraulic press and the texting fixture. With the known cross-sectional area of the specimen through cross-sectional microscopy and its corresponding elastic modulus for each material, the flexural stress can be determined.

In a three-point bending test, flexural strain of the specimen is quantified by optically measuring deflection with Basler acA2440- 35μm machine vision camera. Image processing is used to quantify deflection. Simultaneously, a stress-strain curve is generated to identify the mechanical properties and strain induced EL luminance relation is acquired to visualize EL-strain behaviour of the structure.

A 6kHz-108V-DC-AC inverter is used to power the specimen. The EL luminance generated by the specimen is quantified using a camera in 12bit mono mode (Basler acA2440-35μm); a 50mm focal length lens (MVL50M23, Navitar) to capture images at fixed aperture size (f/2.8). To capture EL luminance without influence of ambient lighting, the base of the ASTM D2344 testing fixture is hollow out and connected to a 50mm rectangular sprayed with non-reflective black paint to reduce the error due to reflected light rays. ImageJ is used to quantify the 12-bit mono tiff images to location-grayscale value matrix. And comparing it to a benchmark light source with known luminance output (EL Strip Tape, Adafruit).

3 RESULT AND ANALYSIS

3.1 Experimental Characterization

The EL luminance control parameters for each fabricated components of the structure are quantified.

The resistivity of sheet structures was measured by Van Der Pauw method. With known CF mesh thickness of (33.18μm) and woven CF fabric at 3-ton curing condition of (213.18 μm) according to Figure 6 (a), the resistivity results are shown in Figure 6 (b). Epoxy resin infusion to both electrodes effectively doubles the resistivity, possibly due to encapsulation preventing radial electrical conduction (from filament to filament) for CF filaments.

(a) 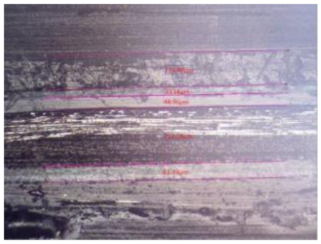

(b)

Resistivity (μΩ·m)	
Woven CF Fabric	
Natural	*Epoxy Resin Infused*
268.7	426.2
Semi-Transparent CF Mesh	
Natural	*Epoxy Resin Infused*
419.7	670.0

Figure 6 (a) 10x Magnification of Cross-sectional microscopy: Thickness of layers are quantified with pixel counting, (b) Resistivity characterization for both woven CF fabric and semi-transparent mesh in natural and epoxy resin infused condition

The surface finish of the epoxy resin infused woven CF lamina is measured with optical profilometry and quantified as surface roughness (Ra). From observation, the surface roughness is directly proportional to the curing condition, namely, the compression force up to the limit of the surface roughness of the compression plate itself. In Figure 7 (a), the optimal compression force is 2 tons, as the surface roughness variation reduces about this load.

As the surface undulation and infill epoxy resin between weft and warp of CF bundle reduces with increase compression force, the woven CF fabric electrode gets closer to the membrane. Inspecting from Figure 10 (a), the CF mesh pattern dominates at 1000kg (1 ton) and woven CF pattern dominates at 2000kg (3 tons), leaving mixed pattern at 2000kg (2 tons). Additionally, the luminance gradient as a function of distance from the voltage source reduces for high compression force. From observation, surface roughness above 62.5μm is not suitable for spin coating uniform membrane and produces non-visible EL luminance according to Figure 7 (b).

(a) 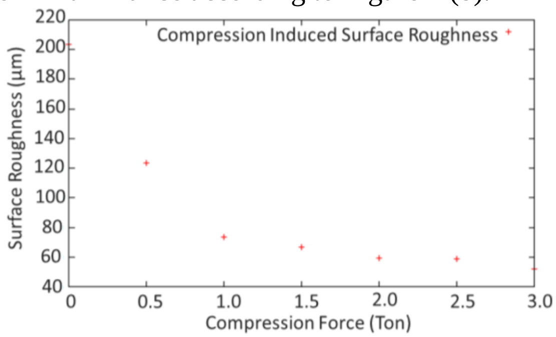

(b) 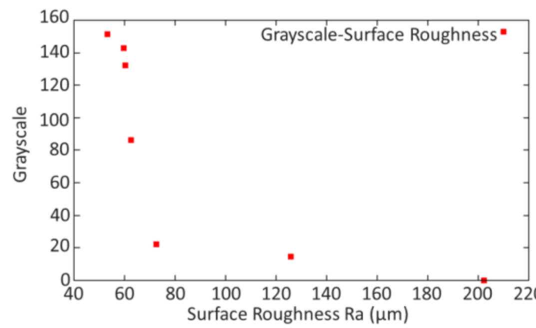

Figure 7 Woven CF lamina Surface Roughness Characterization: (a) Fabrication compression force relation, (b) EL luminance Grayscale relation (Specimen fabricated with thickness of 20.34μm and 50% phosphor infill fraction)

Since the overall device is an EL capacitor, the dielectric phosphor membrane is characterized with two control parameters: *effective dielectric constant* and *membrane thickness* according to Equation 2, where ε_{eff} is the effective relative dielectric constant and t is the thickness of the membrane.

$$C = \varepsilon_0 \varepsilon_{eff} \frac{A_s}{t} \qquad (2)$$

The dielectric phosphor membrane thickness is measured with stylus profilometry and confirmed with cross-sectional microscopy. In Figure 9 (a), the relation between spin coating speed and ZnS: Cu powder filler fraction with membrane thickness is demonstrated. As expected, the membrane thickness decreases with increasing spin speed toward a plateau. The phosphor filler fraction directly influences the viscosity of the mixture, thus the thickness increases increase of phosphor fraction.

The EL luminance increase drastically with decreasing membrane thickness (see Figure 8 (b) and Figure 10(a)) which is inversely proportional to capacitance, and the inverse proportional is confirmed in

Figure 8 (b). Although the luminance has varied greatly, the underlying woven pattern did not change with membrane thickness variation.

(a)

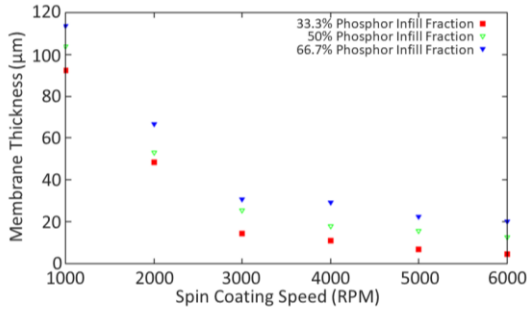

(b)

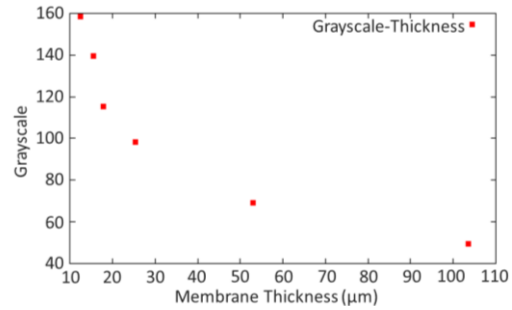

Figure 8 Phosphor Dielectric Membrane Thickness Characterization: (a) fabrication characterization with spin coating speed and phosphor infill fraction, (b) EL luminance Grayscale Relation

In a heterogenous structure, the effective dielectric constant can be expressed by Equation 3, with ε_D and ε_P being the binder and phosphor dielectric constant, and f_P is the phosphor filler fraction. CF (Capacitance-Frequency) and CV (Capacitance-Voltage) sweeps are used to generate the relationship between effective dielectric constant and phosphor filler fraction shown in Figure 9 (a) with control surface area (A_s) and membrane thickness (t). The result is then confirmed with Equation 3. With capacitance measurement on pure epoxy resin membrane, the relative dielectric constant of the 2000/2020 system epoxy resin is determined to be at 5.42. From linear extrapolation, the relative dielectric constant of ZnS: Cu Model D502B is estimated to be 8.25 which is shown to be the dominant dielectric in the ZnS: Cu-epoxy resin membrane.

For dielectric-phosphor ratio varying specimen, the luminance variation effect is as drastic as thickness variation, since ZnS: Cu powder is the dominant dielectric and illuminator. In Figure 9 (b), as phosphor infill fraction drop below 50%, the luminance is not visible to human eye and the current camera setting.

$$\varepsilon_{eff} = \varepsilon_D \left[1 + 3f_P \frac{\varepsilon_P - \varepsilon_D}{\varepsilon_P(1-f_P) + \varepsilon_D(2+f_P)}\right] \qquad (3)$$

(a)

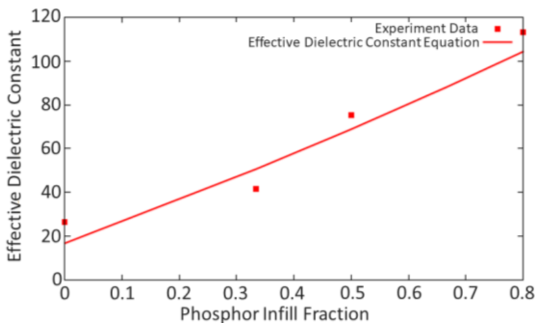

(b)

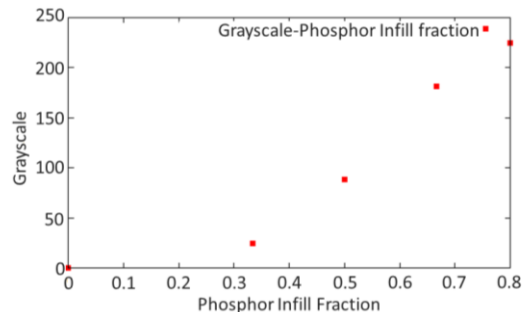

Figure 9 Effective Dielectric Constant Characterization: Fabrication ZnS: Cu Phosphor Infill Fraction Relation, (b) EL luminance as a function of phosphor infill fraction.

3.2 Mechanical Test

The damage state condition in the mechanical test is defined as two categories: *delamination* and *bending crack*. The effect of mechanical testing is shown in Figure 10. This figure demonstrates illumination response due to an input bending stress. The developed sensing structure is capable of detecting delamination and cracking as shown in Figure 10 (b).

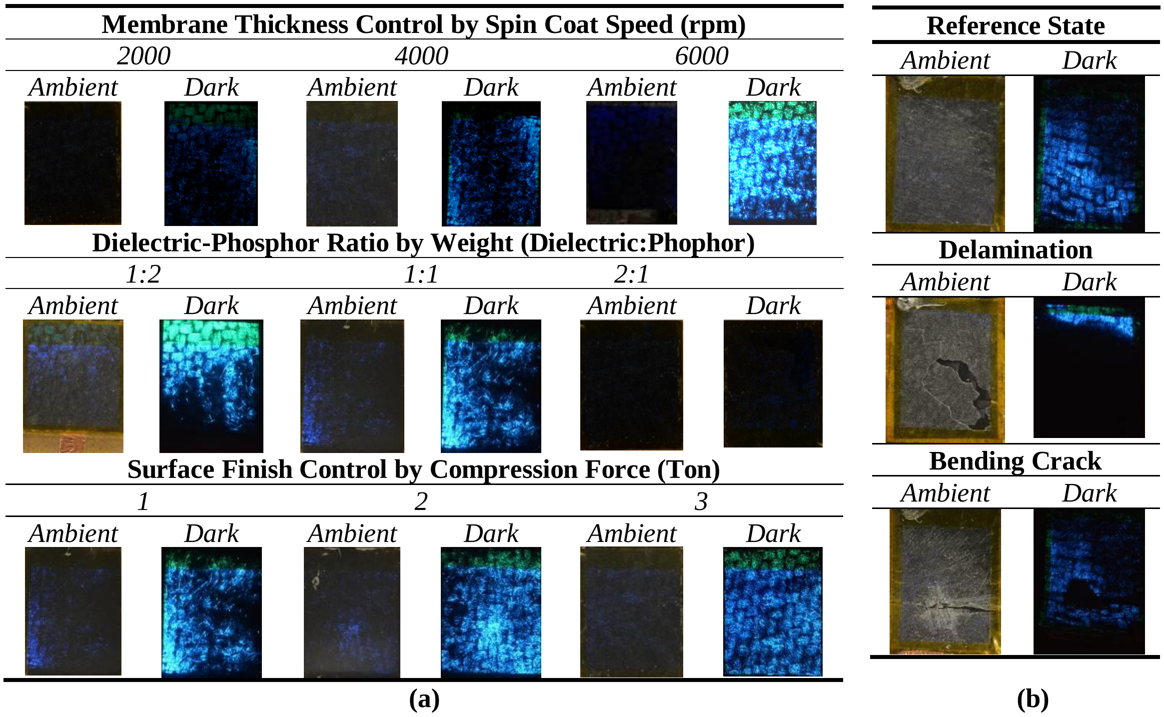

Figure 10 EL Test: (a) Characterization Samples of ZnS: Cu - epoxy resin membrane by control membrane thickness, dielectric-phosphor ratio, and surface finish captured in both ambient lighting and darkroom condition; (b) Damage state EL luminance detection in Delamination and Bending Crack

CONCLUSIONS

SHM and visualization utilizing a novel ACEL CF composite structure is demonstrated. The proposed fabrication process is compatible with traditional composites manufacturing. Optimized fabrication and device parameters are presented to maximize luminescent output. Damage in the CF structure due to bending can be clearly observed with variations in luminescence.

REFERENCES

Bilisik K. 2017. “Characterizing the Deformation of Woven Textile Composites.” *SPE Plastics Research Online* (September):1–3.

Cai, Jian, Lei Qiu, Shenfang Yuan, Lihua Shi, PeiPei Liu, and Dong Liang. 2012. “Structural Health Monitoring for Composite Materials.” *Composites and Their Applications* (August):36–60.

Laminates, Their. 2000. “ASTM D2344 for Short Beam Strength.Pdf.” 03.

Lang, Eric J. and Tsu Wei Chou. 1998. “The Effect of Strain Gage Size on Measurement Errors in Textile Composite Materials.” *Composites Science and Technology* 58(3–4):539–48.

Liang, Guojin, Ming Yi, Haibo Hu, Ke Ding, Lei Wang, Haibo Zeng, Jiang Tang, Lei Liao, Cewen Nan, Yunbin He, and Changhui Ye. 2017. “Coaxial-Structured Weavable and Wearable Electroluminescent Fibers.” *Advanced Electronic Materials* 3(12):1–10.

Xia, Z. H. and W. A. Curtin. 2008. “Damage Detection via Electrical Resistance in CFRP Composites under Cyclic Loading.” *Composites Science and Technology* 68(12):2526–34.

Zhu, Ji Hua, Miaochang Zhu, Ningxu Han, Wei Liu, and Feng Xing. 2014. “Electrical and Mechanical Performance of Carbon Fiber-Reinforced Polymer Used as the Impressed Current Anode Material.” *Materials* 7(8):5438–53.

Zhu, Yong Kai, Gui Yun Tian, Rong Sheng Lu, and Hong Zhang. 2011. “A Review of Optical NDT Technologies.” *Sensors* 11(8):7773–98.